Trapping, corralling and spectral bonding of optical resonances through optically induced potentials

PETER T. RAKICH*, MILOŠ A. POPOVIĆ, MARIN SOLJAČIĆ AND ERICH P. IPPEN

Research Laboratory of Electronics, Massachusetts Institute of Technology, 77 Massachusetts Avenue, Cambridge, Massachusetts 02139, USA
*e-mail: rakich@mit.edu

Published online: 1 November 2007; doi:10.1038/nphoton.2007.203

Optical forces resulting from interacting modes and cavities can scale to remarkably large values as the optical modes shrink to nanometre dimensions. Such forces can be harnessed in fundamentally new ways when optical elements can freely adapt to them. Here, we propose the use of optomechanically coupled resonators as a general means of tailoring optomechanical potentials through the action of optical forces. We show that significant attractive and repulsive forces arising from optomechanically coupled cavity resonances can give rise to strong and highly localized optomechanical potential wells whose widths can approach picometre scales. These potentials enable unique all-optical self-adaptive behaviours, such as the trapping and corralling (or dynamic capture) of microcavity resonances with light. It is shown, for example, that a resonator can be designed to dynamically self-align (or spectrally bond) its resonance to an incident laser line. Although these concepts are illustrated through dual-microring cavity designs, broad extension to other photonic topologies can be made.

The first measurements of radiation pressure provided a glimpse into how optical fields can manipulate mechanical structures[1]. Technological advances and nanometre-scale lithography have since enabled fundamentally new ways to confine and manipulate light on a chip[2–5], enabling the scaling and enhancement of numerous physical effects[6–8]. In particular, it has been noted that the remarkable spatial confinement and large field enhancements afforded by nanometre-scale guided modes can result in significant forces when optical modes and cavities interact[9,10]. Such observations have sparked further theoretical interest[11–13], and recent experiments have shed light on the experimental utility of such forces for future integrated photonic systems[14]. In this paper, we propose the use of microcavity resonances as a general means of synthesizing optomechanical potentials through the action of optical forces. We show that these synthesized optomechanical potentials enable unique designs for all-optical functionalities when photonic elements are allowed to freely adapt in response to these potentials. The result is a new class of self-adaptive photonic devices that facilitate 'corralling' and 'trapping' of microcavity resonances with light.

Extending this concept, we show that it is feasible to construct a cavity that dynamically self-aligns to the incident laser frequency through spectral bonding of the cavity resonance to that of the incident laser line. This bound state can be used to tune and manipulate the cavity resonance over extensive wavelength ranges, which would be difficult by any other means. Furthermore, when multiple laser lines are used, the cavity resonance can be manipulated and placed at virtually any frequency all-optically. Finally, because this resonance frequency control corresponds to picometre-level positional control of membranes and cantilevers, this concept also shows great promise as a means for nanomechanical control in nanoelectromechanical systems (NEMS) and microelectromechanical systems (MEMS).

In what follows, we consider resonator topologies that facilitate resonant-mode-based potential synthesis, leading to optomechanical cavity-trapping and self-adaptive optical microcavities through spectral bonding. Although the examples presented are cast in terms of microring cavities, the concepts described are quite general, and can be readily applied to a host of cavity topologies.

RESULTS

PROPOSED APPROACH AND DEVICE TOPOLOGY

The design in Fig. 1a enables mechanically variable strong coupling between two microring cavity modes. It is assumed that the separation, q, between the microrings is a free variable such that the equilibrium position of the system is dictated solely by the optically induced potentials. Close approximations of this arrangement can be realized using membrane or cantilever structures to suspend the upper ring, and could be achieved using available fabrication techniques[15,16]. As the separation, q, between the microrings is decreased (and optical coupling increased) large splitting of the natural (symmetric and antisymmetric) cavity modes is produced. For large enough coupling, this generates resonance crossings between distinct resonant orders. We show that this strong resonator coupling and these resonance crossings facilitate the creation of localized minima of optomechanical potential, which lead to a fundamentally new means of controlling optical elements

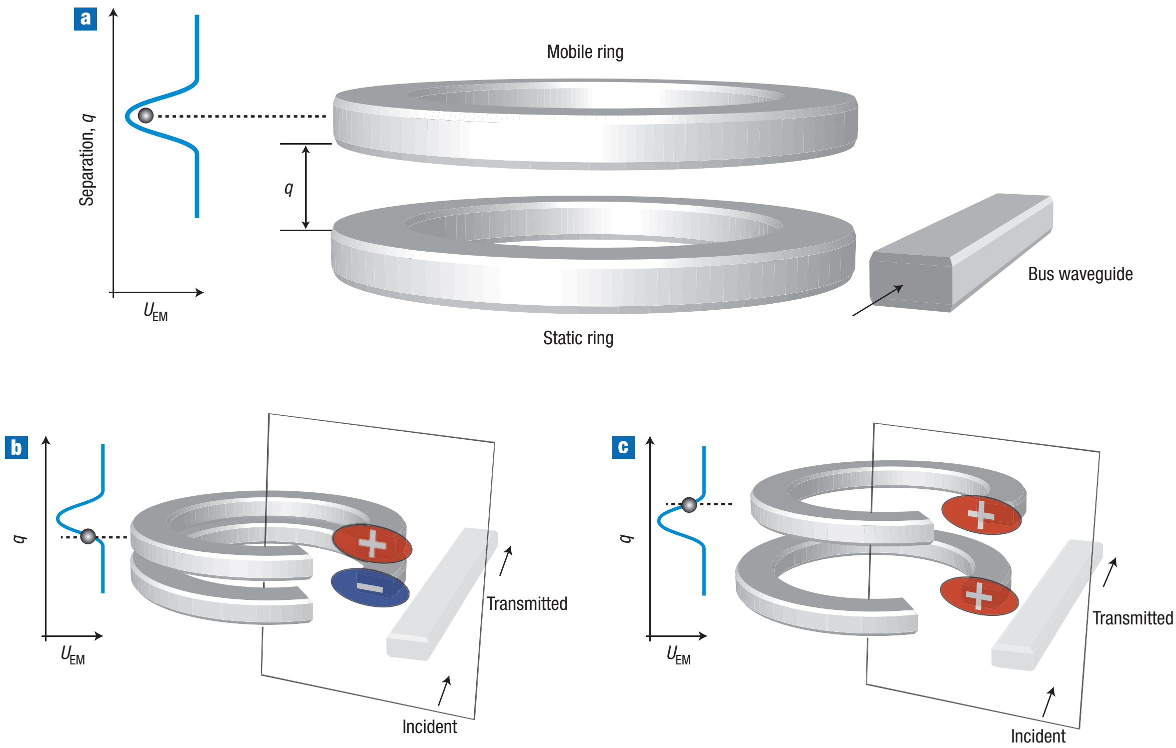

Figure 1 Optomechanically coupled dual-cavity structure under optical excitation. **a**, Optomechanical system shown in its trapped state, corresponding to a minimum of effective optomechanical potential. **b**,**c**, Representation of how the modes of the dual-ring structure create a potential well. The correspondence of the repulsive (antisymmetric) (**b**) and attractive (symmetric) (**c**) ring modes are shown with respect to positions on the potential well (dotted lines connect the illustrated ring separation to that of the sketched total potential). Under monochromatic excitation, the symmetric and antisymmetric modes become resonant for different positions, q, yielding a localized resonantly synthesized potential well of this form.

through resonantly bound optomechanical states. These unique bound optomechanical states make trapping, corralling and self-adaptive spectral bonding phenomena possible.

Trapping and manipulation, of the type we seek, requires the synthesis of a minimum in potential energy for the optomechanical system. Thus, a necessary condition for trapping is that both attractive and repulsive forces occur. A closed-system analysis of an optical cavity presents a straightforward way to understand what is required to generate attractive and repulsive forces (Fig. 1b,c). Therefore, we begin by identifying the essential behaviour of this cavity system through the conventional closed-system analysis of forces before we formulate an open-system analysis, enabling direct evaluation of the potential energy.

CLOSED-SYSTEM ANALYSIS OF CAVITY TRAPPING

Through the closed-system analysis it is assumed that the cavity system does not couple to the outside world (that is, the fractional power coupling γ between the ring and bus waveguides, as seen in Fig. 1a, is zero, and is treated as a lumped coupling through a scattering matrix formalism[17]), and the number of photons (N) within the dual-ring system remains fixed. Therefore, the energy of the closed-system cavity is $U^{c}_{EM} = N\hbar\omega$, where $\hbar$ is the reduced Planck's constant, and ω is the photon frequency. Thus, a change of cavity geometry resulting in a positive frequency shift ($\delta\omega > 0$) increases the system energy, and a negative shift ($\delta\omega < 0$) lowers the system energy. In the context of dielectric waveguides and cavities, the change in frequency relates to the change in effective index (δn) and the group index (n_g) of the waveguide mode through the relation $\delta\omega/\omega = -\delta n/n_g$ (ref. 18). Therefore, if a change of cavity geometry, δq, can produce either $\delta n > 0$ (that is, $\delta\omega < 0$) or $\delta n < 0$ (that is, $\delta\omega > 0$), both signs of force can be achieved.

As a means of achieving both attractive and repulsive forces, we focus on the symmetric and antisymmetric guided modes of the dual-ring structure illustrated in Fig. 2a. For a change of waveguide geometry, $\delta q < 0$, symmetric modes exhibit $\delta n > 0$ (that is, attractive forces), and antisymmetric modes exhibit $\delta n < 0$ (that is, repulsive forces)[9,10]. The cross-section of the dual-ring resonator with examples of computed symmetric and antisymmetric transverse electric (TE)-like guided modes is shown in Fig. 2a–c. We assume core and cladding refractive indices of 3.5 and 1, respectively. In this symmetric waveguide configuration, the effective indices of the coupled guided modes (that is, supermodes) are $n_{\pm} = n_0 \pm \kappa(q)$, as computed through first-order coupled-mode theory[17,19]. The symmetric mode corresponds to n_+, and the antisymmetric mode corresponds to n_-. Here, $\kappa(q)$ is the waveguide coupling strength (in radians per metre) normalized by the free-space wavenumber, $2\pi/\lambda$, which takes on an exponential dependence with waveguide separation, q. A plot of the computed effective index versus waveguide separation is shown in Fig. 2d for the waveguide geometry of Fig. 2a, revealing the expected symmetric splitting with increasing κ (or decreasing q).

Using the structure of the guided modes, we can analyse the resonance frequencies of the coupled dual-ring system. The ring cavity develops symmetric and antisymmetric resonant cavity modes (see Fig. 1b,c), corresponding to the symmetric and antisymmetric waveguide modes seen in Fig. 2b,c. Therefore,

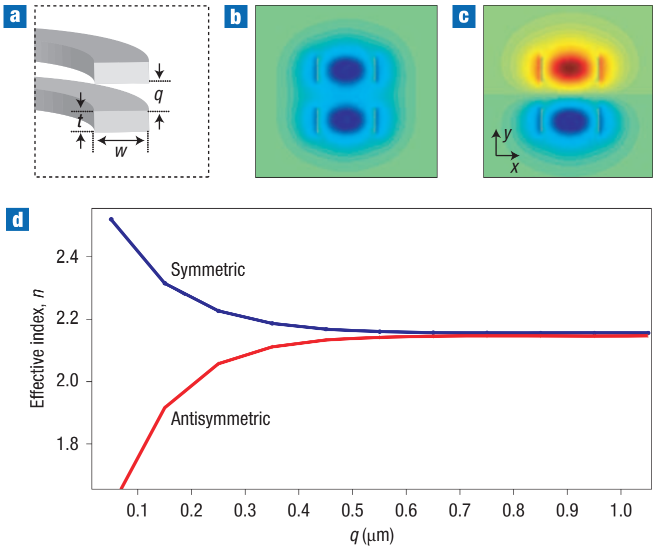

Figure 2 Modal analysis of the dual-ring strucure. a, Cross-section of dual coupled rings with a core refractive index of 3.5, a cladding refractive index of 1, and dimensions $w =$ 500 nm, $t =$ 200 nm and $q =$ 250 nm. **b**,**c**, Colour map showing the x-component of the electric field for symmetric (**b**) and antisymmetric (**c**) modes of the waveguide for $\lambda = 1.55$ µm. **d**, Computed effective index of symmetric and antisymmetric modes for waveguide cross-section in **a** as q is varied.

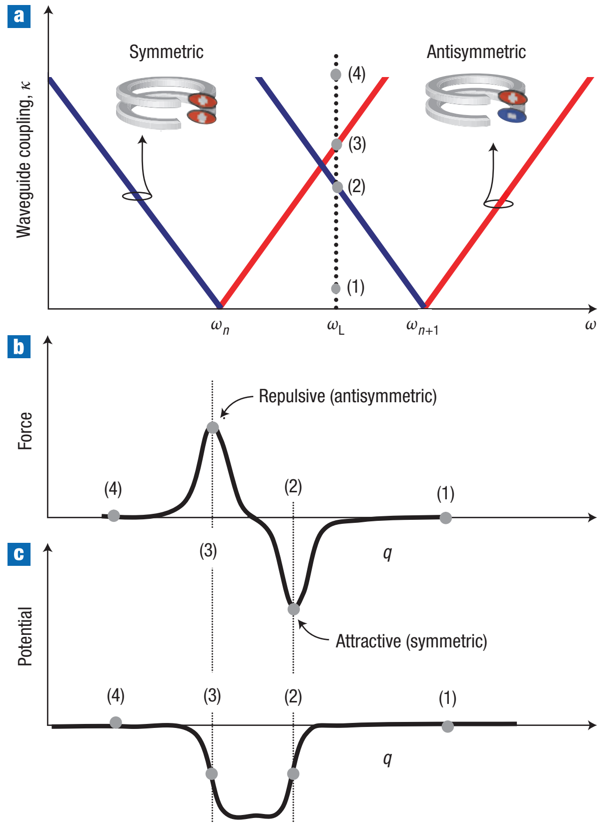

Figure 3 A conceptual outline of cavity trapping. a, A sketch of the resonance frequencies, ω, of the symmetric (blue) and antisymmetric (red) microring cavity modes as the waveguide coupling strength κ is varied. Symmetric splitting of the symmetric and antisymmetric modes is found in this plot. **b**, A sketch of the forces versus ring–ring separation, q, for a fixed laser line excitation indicated by the vertical dotted line in **a**. **c**, The effective potential corresponding to the forces shown in **b**.

the mth-order symmetric and antisymmetric resonances will occur at frequencies

$$\omega_{\pm}^{m}(\kappa) \cong \omega_m \mp \left(\frac{\omega_m \cdot \kappa(q)}{n_g}\right). \quad (1)$$

From the preceding analysis, we see that excitation of the symmetric cavity mode results in attractive forces, whereas excitation of the antisymmetric mode (with a frequency shift of opposite sign) results in a repulsive force.

Notably, through this dual-ring geometry, the waveguide coupling strength (κ) can be large enough to tune a microring of realistic dimensions across multiple resonance orders. For instance, a microring with this cross-section (consistent with $n_g \simeq 4$) and a radius of 2.5 µm will possess a free spectral range (FSR) of about 4.5 THz (that is, ~40 nm centred at $\lambda \sim$ 1,550 nm). In this case, equation (1) (and Fig. 2d) tell us that it should be feasible to tune our cavity resonance through a frequency range of greater than 45 THz. In this strong coupling regime, we observe degenerate crossing of the cavity modes from different FSRs. Figure 3a illustrates the resonance splitting that equation (1) would lead us to expect. Although there will probably be multiple frequency crossings, we sketch only the first cavity crossing in Fig. 3a.

So far, our closed-system analysis assumes zero power coupling (γ) between the bus waveguide and ring system shown in Fig. 1a. However, even if $\gamma \neq 0$, the symmetric (attractive) and antisymmetric (repulsive) modes can be excited with similar efficiencies when the incident light is resonant with the corresponding mode. The resulting attractive and repulsive forces generated between the rings will be proportional to the intracavity power (or photon density) of the respective mode. This follows from the equivalence of the computed forces found through integral methods and the closed-system analysis (see Methods). Therefore, if a monochromatic laser line is used to excite this system through the bus waveguide, resonantly induced attractive and repulsive forces will be produced at various positions cornma, q, corresponding to resonant alignment of the cavity mode with the laser frequency.

Using the intuition derived from the closed-system analysis, we begin by examining the case when the resonant system is excited with a fixed laser line (at frequency ω_L) that is blue-detuned from the resonance crossing, as illustrated by the vertical dotted line in Fig. 3a. In the limit of small κ (or large q), the cavity modes are nearly degenerate, and at their natural frequencies. In this case (illustrated by point (1) in Fig. 3a–c), the laser line is detuned from all resonances of the system (that is, forces are negligible). As we increase the ring–ring coupling (or decrease q), we will resonantly excite the symmetric cavity mode (indicated by point (2) of Fig. 3a–c) as it shifts to lower frequencies, followed by the antisymmetric cavity mode (indicated by point (3) of Fig. 3a–c) of a lower resonant order as it shifts to higher frequencies. Excitation of the antisymmetric mode results in repulsive forces between the rings, and the symmetric mode results in attraction. Hence, the force versus ring–ring separation is as shown in Fig. 3b. These forces correspond to the effective potential presented in

Fig. 3c. Therefore, we see that for blue-detuning from a resonance crossing, it is feasible to trap the upper (mobile) ring such that the laser excitation remains resonant, or nearly resonant, with both cavity modes (also illustrated in Fig. 1b–c). This is what we refer to as state trapping of the optomechanical system's resonance.

OPEN-SYSTEM EVALUATION OF CAVITY TRAPPING

The effective potential of the coupled system is the salient information required to predict the physical behaviour of optomechanical cavity trapping. Although the closed-system view can be adapted to provide a rigorously valid means of deriving the force in an open system, an alternative view explicitly deriving the potential for an open system provides simplicity and insight for the discussion of trapping. We show that the potential of a lossless open system, such as this one, is directly proportional to the phase ϕ that the cavity imparts on the transmitted field in the bus waveguide. For a steady-state monochromatic excitation (of fixed frequency), the work done by the cavity on the transmitted laser radiation is given by $\Delta U^{\mathrm{o}}_{\mathrm{EM}} = -\Phi\hbar\Delta\phi(q)$ (see Methods). Here, Φ is the incident photon flux and $\Delta\phi(q)$ is the phase change induced on the transmitted wave as q is varied from $q_{\mathrm{i}} = \infty$ to $q_{\mathrm{f}} = q$. Therefore, $\Delta U^{\mathrm{o}}_{\mathrm{EM}}$ is the effective potential of the optomechanical system at the steady state. (For further details see Methods.)

For the purposes of our first example, we assume a ring circumference L of 16 μm, a fractional power coupling γ of 0.10 (or 10%) between the bus waveguide and the microring, and the ring cross-section previously described. We can locate the cavity resonances by identifying the frequencies where the round-trip phase is an integer multiple of 2π, or $\beta_{\pm}L = (\omega/c)n_{\pm}L = 2\pi m$. Here, β is the propagation constant, c is the speed of light in vacuum and m is an integer corresponding to the resonance order. Tracking the resonances of the cavity for all values of κ and ω, we obtain the rigorous solution of Fig. 4a, similar to the generic illustration in Fig. 3a. Note that each row of resonance crossings occurs for an integer difference in resonance order of the symmetric and antisymmetric modes.

To evaluate the potential energy of this system when illuminated by a laser line, we must compute ϕ of the transmitted field amplitude as a function of ω and κ. Through use of spatial coupled-mode theory[17,19] and the scattering matrix formalisms[17,20,21], the phase response of the dual-ring system can be readily computed in a rigorous manner. At large enough detuning from a mode crossing, one finds that the system is nearly equivalent to a cascade of two resonant modes (symmetric and antisymmetric), spatially co-located, where the spectral linewidth of each is determined by the external coupling to the bus waveguide. However, the spatial resolution of the trapping potential produced by this system is not limited by the linewidth of the individual resonator modes as set by coupling to the bus waveguide. This is because for frequencies approaching the resonance crossing, with a detuning smaller than the linewidth, interference of the symmetric and antisymmetric resonances gives rise to a narrow linewidth supermode.

Based on this model, the potential energy of the optomechanical system can be computed for various forms of optical excitations. For example, see the computed normalized potential energy, $\Delta U_{\mathrm{EM}}/(\hbar\Phi)$ (also equal to the potential energy at $-\phi$), as a function of κ and ω, as shown in Fig. 4b. If a laser excitation is assumed to be blue-detuned from the cavity mode crossing ($\omega_{\mathrm{L}} = 200$ THz, shown by the vertical line in Fig. 4a), we have the effective potential indicated by the solid black line on the surface plot of Fig. 4b. As expected from our earlier conceptual analysis, minima of potential occur when blue-detuned from the resonance crossing. This means that the optomechanical system will be trapped at discrete locations in space, effectively pinning the optomechanical system at a position q that is midway between the symmetric and antisymmetric resonances (that is, exciting the symmetric and antisymmetric resonances equally).

Moreover, if a single laser line frequency is continuously swept towards the resonance crossing (over the trajectory shown by laser lines as indicated by solid lines (1) to (3) in Fig. 4c) we can adiabatically narrow the potential from a wide square-well to a δ-function, effectively allowing us to corral the system to one of several localized positions in space, corresponding to resonance orders of the microcavity. The evolution of the potential for three different wavelengths can be seen in Fig. 4e for a realistic guided power of 1 mW within the bus waveguide (or $\Phi \approx 1 \times 10^{16}$ photons per second). For these modest powers, we see that the depth of the potential well is tens of electron volts (eV).

In the limit of small detuning from the resonance crossing, the spatial localization of the trapping potential scales to arbitrarily narrow values. For example, Fig. 4f reveals that the width of the trapping potential shrinks to 1 pm (in space) as the detuning from the resonance crossing approaches zero. This high level of spatial localization is made possible by the fact that, as detuning becomes smaller than the linewidth, interference of the two resonances gives rise to a narrow linewidth supermode. These spectrally narrow features translate to a sharper rise and fall of the potential (in space), making a high degree of localization possible. As the mode crossing is approached, the trapping potential narrows, and the finite linewidth of the resonator modes leads to a shallowing of the potential. However, the potential does not vanish and asymptotically approaches a 50% depth at large detunings.

Additionally, cavity modes can be manipulated in a much more arbitrary fashion when two independent laser lines are used. For instance, if laser lines are placed asymmetrically about the resonance crossing, as illustrated by laser lines (1) and (2) on the surface map of Fig. 4d, the potential experienced by the cantilever will be a result of both laser lines. The total potential that the cantilever experiences, as a result of both laser-line excitations, is shown in Fig. 4g. A unique minimum of potential will occur for $\kappa = 0.028$ (or $q \approx 350$ nm). Note that this trapping scheme is helped by the fact that the potential is not symmetric in coupling owing to the gradual wavelength dependence that is typical of waveguide coupling strength κ.

PRACTICAL CONSIDERATIONS

Through these schemes, the cavity frequency (and coordinate q) can be pinned to virtually any chosen frequency, corresponding to a continuum of positions. As the trapping potential corresponds to a dimension of ~1 pm in space, a cantilever or membrane that suspends this ring will be stabilized to this subatomic positional level. As one application, this mechanism enables direct tuning and manipulation of the cavity that we excite, with a high degree of stability. This is important, because it has been noted that optical tuning by structural perturbation in nanophotonic structures requires nanometre to picometre levels of control, making other (electromechanical) means of control very difficult to implement[22].

We also note that the depth of the potential generated by this approach is far greater than $k_{\mathrm{B}}T$ (~25 meV at room temperature) meaning that thermal fluctuations are not sufficient to liberate the trapped microring from this remarkably localized potential (here k_{B} and T represent the Boltzmann constant and

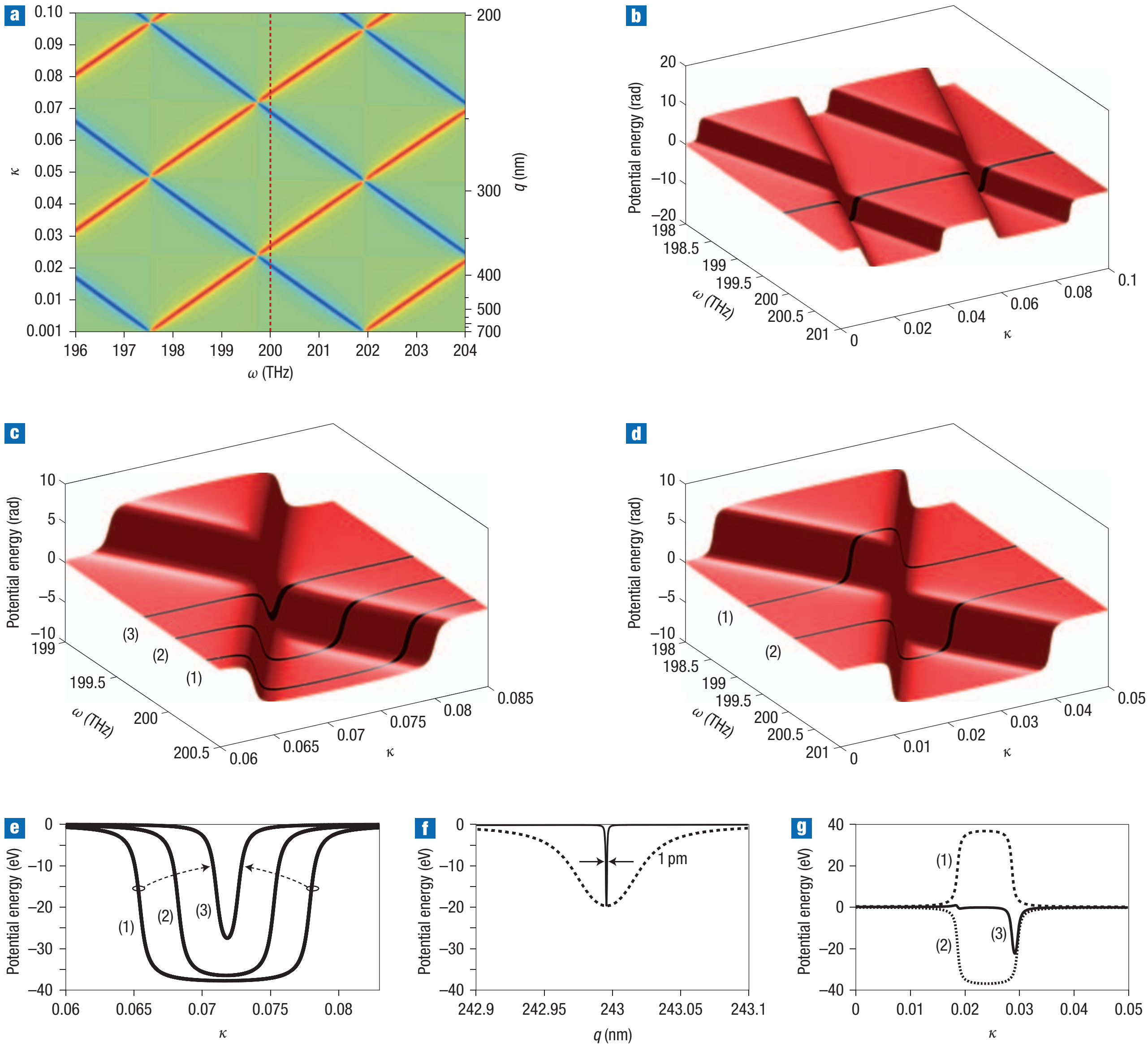

Figure 4 Computed modes and optomechanical potentials of a dual-ring cavity. **a**, Map of symmetric (blue) and antisymmetric (red) cavity modes versus frequency, ω: normalized waveguide coupling strength κ (left axis) and separation q (right axis). **b**, Surface plot of the normalized potential, $U_{EM}/(\Phi\hbar)$ (radians) versus frequency and coupling strength. **c**,**d** Surface maps showing the same data seen in **b** displayed over smaller ranges (laser lines shown in black). **e**, Potential for laser lines shown in **c** (dotted arrows indicate evolution of potential as the laser line is tuned). **f**, Potential versus q for relative frequency detunings of 2.8×10^{-7} (dashed) and 1×10^{-10} (solid). **g**, Total potential from laser lines in **d**. In **e**–**g** 1 mW of incident power is assumed.

temperature respectively). Moreover, forces corresponding to these potentials are large (1–10 μN) compared with gravitational forces of the order of nN and the restoring forces typically generated by micrometre-scale cantilevers and membranes (for example, structures with spring constants ranging from 1×10^{-5} N m^{-1} to 1 N m^{-1}; see refs 14, 23). Short-range interactions such as van der Waals and capillary forces need not significantly affect the operation of such devices if the distance q between interacting surfaces is kept greater than approximately 20 to 30 nm (corresponding to the retarded regime of van der Waals interaction)[23–27]. Although van der Waals interactions could dominate for smaller distances (depending on surface roughness, geometry, and the Hamaker constant of the interacting bodies), they typically diminish to levels of the order of nN for nonpolar materials at these length scales[25–27]. Therefore, it is feasible to control the perturbing structure with only optical interactions, as these can dominate in experimentally realistic situations.

Finally, although losses were neglected in the preceding analysis, none of these results will be significantly modified if a loss-Q of greater than 1×10^6 (consistent with computed bending losses[28]) is assumed. In practice, excess losses limiting the Q of this system could result from azimuthal asymmetries and surface roughness, and would translate to a diminished level of achievable confinement for the synthesized trapping potential. However, it can be shown that this system is relatively robust to vertical asymmetries (resulting in a frequency mismatch between the rings).

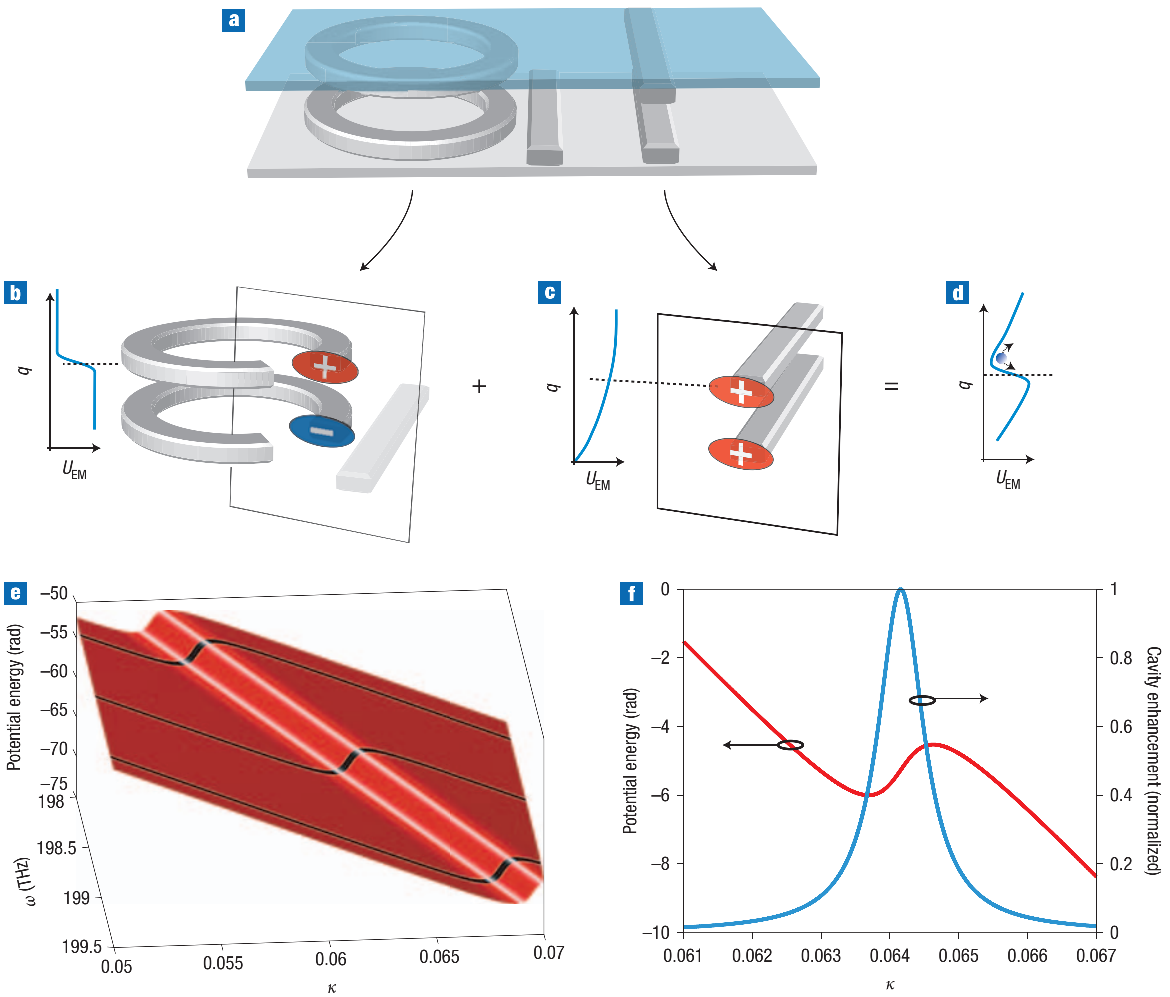

Figure 5 Design for dynamically self-aligning microcavity resonator. a, Self-aligning resonator combining both resonant and non-resonant potentials. **b**, Step-like potential corresponding to excitation of the antisymmetric cavity mode. **c**, Uniform attractive potential corresponding to symmetric coupled waveguides (of similar cross-section). **d**, Sum-total of effective potential generated by resonant and non-resonant potentials, revealing a minimum of potential at the antisymmetric cavity resonance. **e**, A surface map of the normalized effective potential versus frequency (THz) and waveguide coupling strength. **f**, A plot displaying position of the potential minimum with respect to the antisymmetric cavity resonance.

EXAMPLE OF A SELF-ALIGNING CAVITY

So far, we have shown how resonant-mode potential synthesis can be used to create a potential well, and to control a microcavity resonance through all-optical means. Next, we illustrate precisely how these concepts can be applied to integrated photonic systems to generate fundamentally new functionalities. The general approach is broad, and we demonstrate it here with an example structure that adapts its resonance frequency to follow a single incident laser line, all-optically. The result is a frequency-tracking resonator—the first of its kind—whose basic design is shown in Fig. 5a.

The open-system analysis of the effective potential (ΔU^{o}_{EM}) already introduced shows that, as the potential is proportional to the phase response of the system, resonant excitation of the antisymmetric ring mode results in a step-like repulsive potential in the neighbourhood of its resonance (see, for example, Fig. 5b). Therefore, by adding a linear (non-resonant) attractive potential (as shown in Fig. 5c) to that of the antisymmetric cavity resonance, a localized minimum of potential (such as seen in Fig. 5d) can be formed, pinning the optomechanical system to be nearly on-resonance with the antisymmetric mode. (Note that for some subset of ω and κ, the antisymmetric mode is the only resonant mode—for instance, see Fig. 4a—and can therefore be selectively excited.) A linear potential in κ (exponential in q) of this form can be generated by optomechanically variable dual waveguides, such as those seen in Fig. 5c. Our phase formulation of the potential demonstrates that a symmetric waveguide mode will generate a linear effective potential given by $\Delta U^{o}_{EM} = -\Phi_{wg}\hbar(\omega/c)\kappa L_{wg}$, where Φ_{wg} is the photon flux within the symmetric mode of the dual waveguides, and L_{wg} is the effective interaction length of the optomechanically variable portion of the waveguides.

Therefore, if both types of perturbation are achieved synchronously (by the same perturbing structure), the total potential of this system can be of the form seen in Fig. 5e. Figure 5e shows a surface plot of the potential energy of this combined system over a range of laser frequencies (which is a subset of those shown in the resonance map of Fig. 4a).

(Here, $\gamma = 0.1$, and the dual waveguides are assumed to be 100 μm long, with a photon flux that is eight times greater than the bus waveguide.) It can be seen that the shape of this new trapping potential is preserved as the frequency of excitation is varied. This is because the exponential dependence of the waveguide and microring coupling strengths, $\kappa(q)$, have been engineered to be equal. In this case, the trapping potential can be translated spectrally over a range of laser frequencies in a continuous fashion, while maintaining resonant frequency alignment with the antisymmetric mode. As the potential well induced by the laser line generates a bound optomechanical state that tracks the cavity resonance, passive frequency-tracking of the laser line is achieved by the cavity as the laser frequency is adiabatically tuned.

APPLICATIONS AND POSSIBLE IMPLICATIONS

Systems of this type may find applications as self-aligning filters, frequency domain saturable absorbers, or a range of other self-adaptive devices. Figure 5f illustrates the relative alignment of the potential minimum with the cavity resonance as the laser frequency is changed. The frequency offset of the potential minimum from the cavity resonance remains a constant as the laser line is tuned over all wavelengths shown. With this structure, the cavity resonance can be made to track the laser line over the entire 4.5 THz FSR of the microcavity (or ~40 nm in wavelength). Furthermore, if larger FSR cavities, such as photonic-crystal microcavities[2,12], are used, the cavity resonance can be manipulated over wavelength ranges of hundreds of nanometres through all-optical means[12,18].

This example illustrates, for a very simple case, how resonant synthesis of potentials can be used to produce spectral bonding of a cavity mode and the incident laser line (that is, passive locking of the cavity resonant frequency and the driving laser frequency). The combined device illustrated in Fig. 5a yields resonant tracking of a microcavity with a laser line, allowing the microcavity to be tuned and stabilized in frequency over large wavelength ranges. More generally, we can use this approach to control separate ('slave') optical devices that are mechanically coupled to the 'master' trapped resonator through the same membrane or cantilever. In such a device, the master cavity would have substantial intracavity field strengths, leading to optical forces, and the slave cavities would have low enough intracavity fields to have no substantial optomechanical forces, acting as purely passive optical systems. Through such schemes, an array of new possibilities arises for all-optical control of systems. As the potentials synthesized by these optomechanically variable circuits facilitate the precise control of nanomechanical membranes and cantilevers, there are a variety of all-optical operations that can be created by this method, ranging from all-optical switching and tuning (for telecom, sensing and imaging applications) to adaptive dispersion and filter synthesis (for applications such as adaptive filtering of laser lines and optical clock recovery).

DISCUSSION

In conclusion, we have proposed the use of microcavity resonances as a general means of synthesizing optomechanical potentials through the action of optical forces. We have shown that these synthesized optomechanical potentials can result in unique designs for all-optical operations on light that would be difficult to achieve by any other means. As first examples of how this concept could be applied, we have shown how all-optical self-adaptive photonic devices can be made to effectively corral and trap microcavity resonances and achieve dynamic self-alignment of a microcavity resonance to a single laser line over very large wavelength ranges. Such devices have the potential to provide all-optical functionality. In the process, they may eliminate limitations related to the extreme sensitivity of microphotonic functionality to structural dimensions. Finally, as the resonance frequency control provided by these trapping schemes corresponds to picometre-level positional control of membranes and cantilevers, this concept also shows great promise as a new means of nanomechanical control for an optically driven analogue to NEMS and MEMS systems, with the potential to respond and adapt at megahertz rates.

METHODS

OPEN-SYSTEM TREATMENT OF POTENTIAL ENERGY

For the case when $\gamma \neq 0$, the ring is no longer a closed system. However, the forces found through a closed-system analysis are correct. This can be seen from the fact that the optical forces produced depend only on the field distribution within the cavities, and can be computed through Maxwell stress-tensor integral methods[9,29]. As equivalent closed- and open-system analyses of the same physical system require similar field distributions within waveguide and cavity modes, it can be shown that the forces found through open-system and closed-system analyses converge to the same value.

Through the open-system analysis, one can go on to show that the change in field energy imparted on the incident monochromatic wave by the lossless all-pass cavity (of the form studied here) can be expressed as $\Delta U^{o}_{EM} = -\Phi\hbar\Delta\phi(q)$. In deriving this result, we consider the interaction of a monochromatic light (of frequency ω_o) with a lossless all-pass filter, shown in Fig. 1a, whose centre frequency is assumed to be a free parameter. Light passing through the bus waveguide, adjacent to the ring, experiences a phase shift (ϕ) in traversing the ring resonator, which can be expressed as

$$\exp[i(kz - \omega_o t)] \rightarrow \exp[i(kz - \omega_o t + \phi)]. \tag{2}$$

The power incident on the ring (through the bus waveguide) is assumed to be a constant. In the classical limit (that is, in the limit of large photon flux), the incident power can be expressed as $P_i = \Phi_i\hbar\omega_o$. As this is a lossless system, no photons are created or destroyed by the cavity (that is, $\Phi_i = \Phi_t = \Phi = \text{constant}$). Thus, the only means by which electromagnetic energy (U_{EM}) can be modified is through a shift in photon frequency. From the phase convention seen in equation (2), it follows that the instantaneous frequency shift on the transmitted light, resulting from a time-dependent phase, $\phi(t)$, will be $\delta\omega = -\dot{\phi}$. Therefore, the incident (P_i) and transmitted (P_t) powers of the system can be written as

$$P_i = \Phi \cdot \hbar\,\omega_o \tag{3}$$

$$P_t = \Phi \cdot \hbar\,(\omega_o + \delta\omega) \tag{4}$$

or, equivalently,

$$P_t = \Phi \cdot \hbar\,(\omega_o - \dot{\phi}). \tag{5}$$

From the above, we see that a time-dependent evolution of the phase must correspond to a time-dependent change of electromagnetic field energy, according to

$$\frac{dU_{EM}}{dt} = (P_t - P_i) = -\Phi \cdot \hbar\,\dot{\phi}. \tag{6}$$

As the cavity frequency ω and the transmitted phase ϕ can both be expressed in terms of the cavity parameter q, one is free to parameterize the motion of the coordinate q, such that $\dot{\phi}$ can be expressed as $(d\phi/dt)=(d\phi/dq)(dq/dt)$.

Through parameterization, a general time-independent form of equation (6) can be found, yielding

$$\frac{dU_{EM}}{dq} = -\Phi \cdot \hbar\,\frac{d\phi}{dq}. \tag{7}$$

Integration of the above expression reveals that $\Delta U^{\mathrm{o}}_{\mathrm{EM}}$ is a state function of the coordinate q, and can be expressed as $\Delta U^{\mathrm{o}}_{\mathrm{EM}} = -\Phi \cdot \hbar \Delta\phi(q)$. It is important to note that this expression for $\Delta U^{\mathrm{o}}_{\mathrm{EM}}$, or equivalently effective optomechanical potential, assumes adiabatic evolution of the coordinate q, such that $|\dot{\phi}| \gg 1/\tau_{\mathrm{p}}$, where τ_{p} is the intracavity photon lifetime. Finally, we note that identical forces are computed through this formulation of the effective potential and those found through closed-system analysis of the equivalent physical system.

Received 11 June 2007; accepted 14 September 2007;
published 1 November 2007.

References

1. Nichols, E. F. & Hull, G. F. A preliminary communication on the pressure of heat and light radiation. *Phys. Rev.* **13,** 307–320 (1901).
2. Song, B.-S., Noda, S., Asano, T. & Akahane, Y. Ultra-high-Q photonic double-heterostructure nanocavity. *Nature Mater.* **4,** 207–210 (2005).
3. Qi, M. *et al.* A three-dimensional optical photonic crystal with designed point defects. *Nature* **429,** 538–542 (2004).
4. Bozhevolnyi, S. I., Volkov, V. S., Devaux, E., Laluet, J.-Y. & Ebbesen, T. W. Channel plasmon subwavelength waveguide components including interferometers and ring resonators. *Nature* **440,** 508–511 (2006).
5. Rakich, P. T. *et al.* Achieving centimetre-scale supercollimation in a large-area two-dimensional photonic crystal. *Nature Mater.* **5,** 93–96 (2006).
6. Altug, H., Englund, D. & Vučković, J. Ultrafast photonic crystal nanocavity laser. *Nature Phys.* **2,** 484–488 (2006).
7. Badolato, A. *et al.* Deterministic coupling of single quantum dots to single nanocavity modes. *Science* **308,** 1158–1161 (2005).
8. Kippenberg, T. J. *et al.* Analysis of radiation-pressure induced mechanical oscillation of an optical microcavity. *Phys. Rev. Lett.* **95,** 033901 (2005).
9. Povinelli, M. L. *et al.* Evanescent-wave bonding between optical waveguides. *Opt. Lett.* **30,** 3042–3044 (2005).
10. Povinelli, M. L. *et al.* High-Q enhancement of attractive and repulsive optical forces between coupled whispering-gallery-mode resonators. *Opt. Express* **13,** 8286–8295 (2005).
11. Mizrahi, A. & Schächter, L. Mirror manipulation by attractive and repulsive forces of guided waves. *Opt. Express* **13,** 9804–9811 (2005).
12. Notomi, M., Taniyama, H., Mitsugi, S. & Kuramochi, E. Optomechanical wavelength and energy conversion in high-Q double-layer cavities of photonic crystal slabs. *Phys. Rev. Lett.* **97,** 023903 (2006).
13. Mizrahi, A. & Schächter, L. Two slab optical spring. *Opt. Lett.* **32,** 692–694 (2007).
14. Eichenfield, M., Michael, C.P., Perahia, R. & Painter, O. Actuation of micro-optomechanical systems via cavity-enhanced optical dipole forces. *Nature Photon.* **1,** 416–422 (2007).
15. In, H. J., Kumar, S., Shao-Horn, Y. & Barbastathis, G. Origami fabrication of nanostructured, three-dimensional devices: Electrochemical capacitors with carbon electrodes. *Appl. Phys. Lett.* **88,** 83104 (2006).
16. Nichol, A. J., Arora, W. J. & Barbastathis, G. Thin membrane self-alignment using nanomagnets for three-dimensional nanomanufacturing. *J. Vac. Sci. Technol. B* **24,** 3128–3132 (2006).
17. Haus, H. A. *Waves and Fields in Optoelectronics* (Prentice-Hall, Englewood Cliffs, New Jersey, 1984).
18. Rakich, P. T. *et al.* Ultrawide tuning of photonic microcavities via evanescent field perturbation. *Opt. Lett.* **31,** 1241–1243 (2006).
19. Chuang, S. L. *Physics of Optoelectronic Devices* (Wiley, New York, 1995).
20. Madsen, C. K. & Zhao, J. H. *Optical Filter Design and Analysis: A Signal Processing Approach* (Wiley, New York, 1999).
21. Okamoto, K. *Fundamentals of Optical Waveguides* (Elsevier Academic, Burlington, Massachusetts, 2006).
22. Nielson, G. N. *Micro-opto-mechanical Switching and Tuning for Integrated Optical Systems*. Thesis, MIT (2004).
23. Sarid, D. *Scanning Force Microscopy: With Applications to Electric, Magnetic, and Atomic Forces* (Oxford Univ. Press, New York, 1994).
24. Van Spengen, W. M., Puers, R. & De Wolf, I. A physical model to predict stiction in MEMS. *J. Micromech. Microeng.* **12,** 702–713 (2002).
25. Israelachvili, J. N. *Intermolecular and Surface Forces* (Academic, London, San Diego, 1991).
26. Maboudian, R. & Howe, R. T. Critical review: Adhesion in surface micromechanical structures. *J. Vac. Sci. Technol. B* **15,** 1–20 (1997).
27. Srinivasan, U., Houston, M. R., Howe, R. T. & Maboudian, R. Alkyltrichlorosilane-based self-assembled monolayer films for stiction reduction in silicon micromachines. *J. Microelectromech. Syst.* **7,** 252–260 (1998).
28. Popovic, M. *Complex-Frequency Leaky Mode Computations Using PML Boundary Layers for Dielectric Resonant Structures*. Proc. of Integrated Photon. Research 2003, Washington, DC, 17 June 2003.
29. Jackson, J. D. *Classical Electrodynamics* (Wiley, New York, 1999).

Acknowledgements

We thank Z. Wang for helpful technical discussions. This work was supported in part by the Army Research Office through the Institute for Soldier Nanotechnologies under Contract No. DAAD-19-02-D0002.

Author contributions

M.A.P. and P.T.R. jointly proposed the concepts for resonant trapping, self-adaptive manipulation and resonant potential synthesis described here.